

Electronic Supplementary Information

Experimental section

Materials: Amorphous boron (B), red phosphorus (P), sodium citrate dehydrate ($C_6H_5Na_3O_7 \cdot 2H_2O$), nitroferricyanide (III) dihydrate ($Na_2Fe(CN)_5NO \cdot 2H_2O$), and Nafion (5wt%) sodium were purchased from Aladdin Ltd. in Shanghai. Para-(dimethylamino) benzaldehyde ($C_9H_{11}NO$), salicylic acid ($C_7H_5O_3$), sodium citrate dehydrate ($C_6H_5Na_3O_7 \cdot 2H_2O$), hydrazine hydrate ($N_2H_4 \cdot H_2O$), sodium hypochlorite (NaClO), sodium hydroxide (NaOH), hydrochloric acid (HCl), ethanol (CH_3CH_2OH), and carbon paper were bought from Beijing Chemical Corporation. The ultrapure water was purified through a Millipore system used throughout all experiments.

Preparation of BP: BP was synthesis through a vacuum-seal strategy. A total weight of 200 mg elements mixture which the molar ratio of B:P was 1:1.2. After vacuum sealing, the silica tube was annealing at 1200 °C in a muffle furnace for 10 h. The BP was prepared well. Moreover, B catalyst was prepared by the same preparation without the presence of P.

Preparation of BP/CP: Carbon paper (CP) was cleaned via brief sonication with ethanol and water for several times. To prepare the BP/CP, 10 mg BP and 40 μ L 5 wt% Nafion solution were dispersed in 960 μ L water/ethanol ($V : V = 1 : 3$) followed by 1-h sonication to form a homogeneous ink. 20 μ L ink was loaded onto a CP ($1 \times 1 \text{ cm}^2$) and dried under ambient condition. The BP/CP working electrode was prepared well.

Characterizations: TEM images were collected on a HITACHI H-8100 electron microscopy (Hitachi, Tokyo, Japan) operated at 200 kV. XPS measurements were performed on an ESCALABMK II X-ray photoelectron spectrometer using Mg as the exciting source. The absorbance data of spectrophotometer were acquired on SHIMADZU UV-1800 UV-Vis spectrophotometer.

Electrochemical measurements: The N_2 reduction experiments were carried out in a two-compartment cell under ambient condition, which was separated by Nafion 117 membrane. The membrane was treated in H_2O_2 (5%) aqueous solution at 80 °C for 1 h and dipped in 0.1 M H_2SO_4 at 80 °C for another 1 h. And finally, the membrane was treated in ultrapure water at 80 °C for 6 h. The electrochemical measurements were conducted on a CHI660E electrochemical analyzer (CH Instruments, China) in a typical three-electrode setup with an electrolyte solution of 0.1 M HCl (30 mL), a graphite rod

and Ag/AgCl (filled with saturated KCl solution) as the counter the reference electrode, respectively. The potentials reported in this work were converted to RHE scale via calibration with the following equation: E (vs RHE) = E (vs Ag/AgCl) + 0.197 + 0.059 × pH. For N₂ reduction experiments, the electrolyte was bubbled with N₂ for 30 min before the measurement.

Determination of NH₃: Concentration of produced NH₃ was spectrophotometrically determined by spectrophotometry measurement with salicylic acid.¹ In detail, 2 ml aliquot of solution was removed from the cathodic chamber, and then added into 2 ml 1.0 M NaOH solution containing C₇H₆O₃ and C₆H₅Na₃O₇·2H₂O (5 wt%), then added 1 ml NaClO (0.05 M) and 0.2 ml Na₂[Fe(NO)(CN)₅].2H₂O (1 wt%) aqueous solution in turn. After standing at room temperature for 2 hours, the UV-Vis absorption spectrum was measured. The concentration of indophenol blue was determined using the absorbance at a wavelength of 655 nm. The concentration-absorbance curves were calibrated using standard NH₄Cl solution with a series of concentrations. The fitting curve ($y = 0.329x + 0.043$, $R^2=0.999$) shows good linear relation of absorbance value with NH₃ concentration by three times independent calibrations.

Determination of N₂H₄: The N₂H₄ presented in the electrolyte was estimated by the method of Watt and Chrisp.² A mixed solution of C₉H₁₁NO (5.99 g), HCl (concentrated, 30 mL) and ethanol (300 mL) was used as a color reagent. Typically, 5 mL electrolyte was removed from the cathodic chamber, after that, added into 5 mL above prepared color reagent and stirring 10 min at room temperature. The absorbance of the resulting solution was measured at 455 nm. The concentration absorbance curves were calibrated using standard N₂H₄ solution with a series of concentrations. The fitting curve shows good linear relation of the absorbance with N₂H₄ concentration ($y = 0.397 x + 0.038$, $R^2 = 0.999$).

Determination of NH₃ yield and FE: The Faradic efficiency (FE) for N₂ reduction was defined as the amount of electric charge used for synthesizing NH₃ divided the total charge passed through the electrodes during the electrolysis. The total amount of NH₃ produced was measured using colorimetric methods. NH₃ yield was calculated using the following equation:

$$\text{NH}_3 \text{ yield} = [\text{NH}_3] \times V / (m_{\text{cat.}} \times t)$$

Assuming three electrons were needed to produce one NH₃ molecule, the FE could be calculated as follows:

$$FE = 3 \times F \times [\text{NH}_3] \times V / (17 \times Q) \times 100\%$$

Where F is the Faraday constant, $[\text{NH}_3]$ is the measured NH_3 concentration, V is the volume of the electrolyte in the cathodic chamber, Q is the total quantity of applied electricity; t is the reduction time; m_{cat} is the loaded mass of catalyst on carbon paper.

Computational details: Spin-polarized density functional theory (DFT) calculations were performed by using the plane wave-based Vienna ab initio simulation package (VASP).^{3,4} The generalized gradient approximation method with Perdew-Burke-Ernzerhof (PBE) functional was used to describe the exchange-correlation interaction among electrons.⁵ The van der Waals (vdW) correction with the Grimme approach (DFT-D3) was included in the interaction between single molecule/atoms and substrates.⁶ The energy cutoff for the plane wave-basis expansion was set to 500 eV and the atomic relaxation was continued until the forces acting on atoms were smaller than $0.01 \text{ eV } \text{\AA}^{-1}$. The BP (111) and (200) surfaces was modeled using a 3×2 slab with four layers (B–P) which the bottom layer is fixed, and are separated by 15 \AA of vacuum. The Brillouin zone was sampled with $2 \times 2 \times 1$ Gamma-center k-point mesh, and the electronic states were smeared using the Fermi scheme with a broadening width of 0.1 eV.

The free energies of the reaction intermediates were obtained by $\Delta G = \Delta E_{\text{ads}} + \Delta \text{ZPE} - T\Delta S + \Delta G(U) + \Delta G(\text{pH})$, where ΔE_{ads} is the adsorption energy, ZPE is the zero point energy and S is the entropy at 298 K. The effect of a bias was included in calculating the free energy change of elementary reactions involving transfer of electrons by adding $\Delta G(U) = -neU$, where n is number of electrons transferred and U is the electrode potential.⁷ In our calculations, we used $U = -0.60 \text{ V}$ (vs. RHE). $\Delta G(\text{pH}) = -k_{\text{B}}T \ln 10 \times \text{pH}$, where k_{B} is the Boltzmann constant, and $\text{pH} = 1$ for electrolyte. In this study, the entropies of molecules in the gas phase are obtained from the literature.⁶

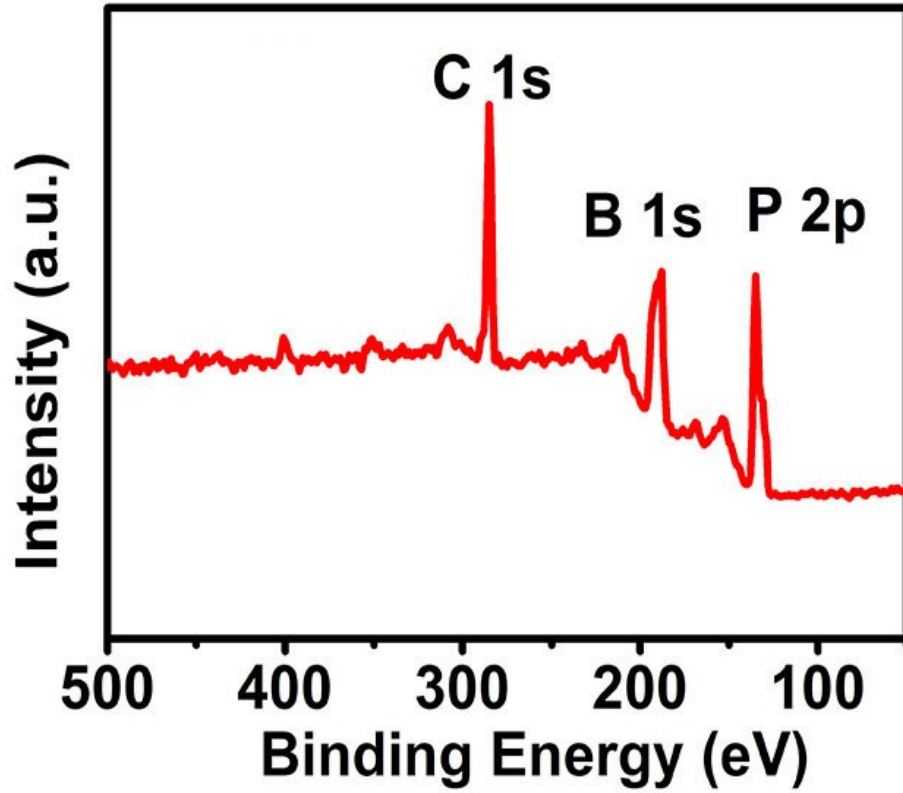


Fig. S1. XPS survey spectrum for BP.

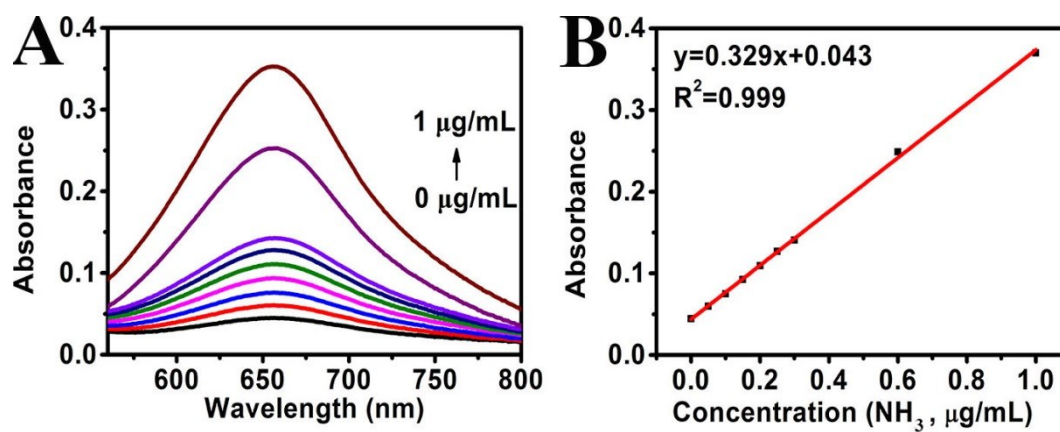


Fig. S2. (a) UV-Vis absorption spectra of indophenol assays with NH_3 concentrations after incubated for 1 h at room temperature in 0.1 HCl. (b) Calibration curve used for calculation of NH_3 concentrations in 0.1 HCl.

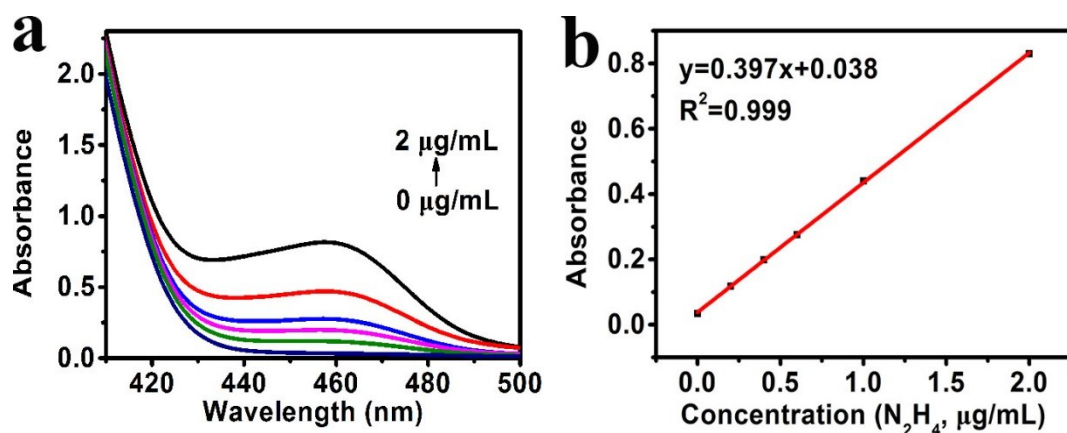


Fig. S3. (a) UV-Vis absorption spectra of N_2H_4 concentrations after incubated for 10 min at room temperature. (b) Calibration curve used for calculation of N_2H_4 concentrations.

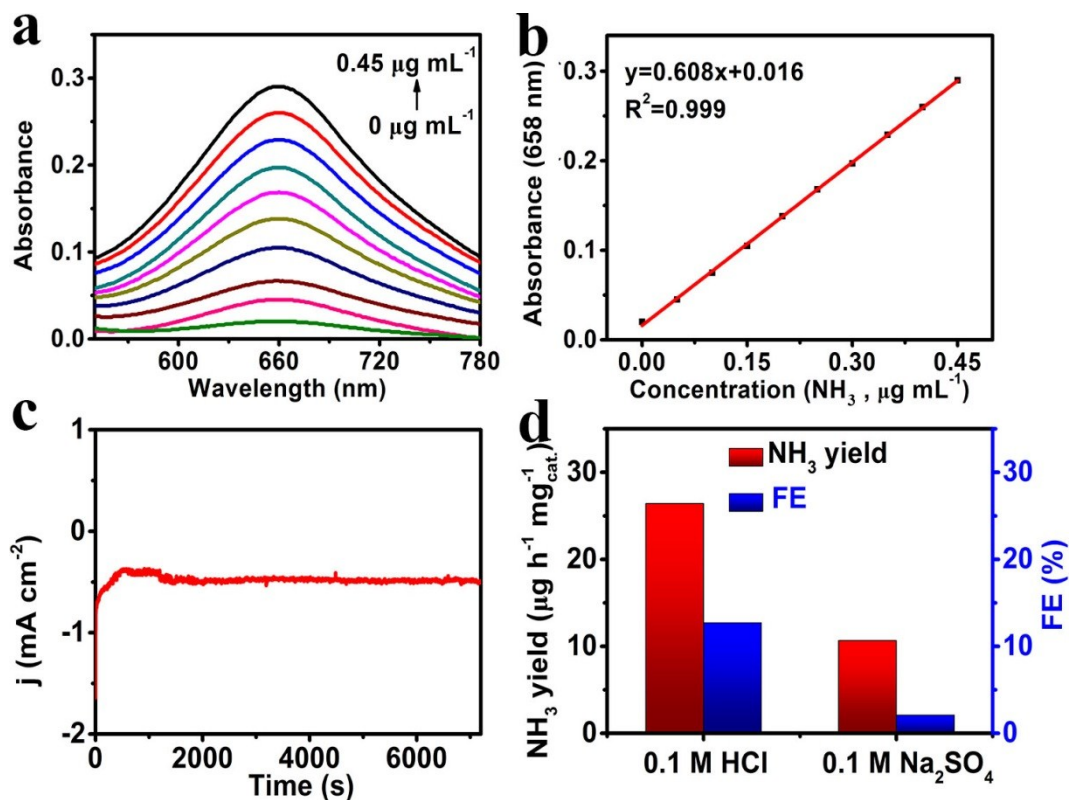


Fig. S4. (a) UV-Vis absorption spectra of indophenol assays with NH₃ concentrations after incubated for 1 h at room temperature in 0.1 M Na₂SO₄. (b) Calibration curve used for calculation of NH₃ concentrations in 0.1 M Na₂SO₄. (c) Time-dependent current density curves over at -0.60 V for 2 h using BP/CP in 0.1 M Na₂SO₄. (d) NH₃ yields and FEs for BP/CP at -0.60 V in 0.1 M Na₂SO₄ and 0.1 M HCl.

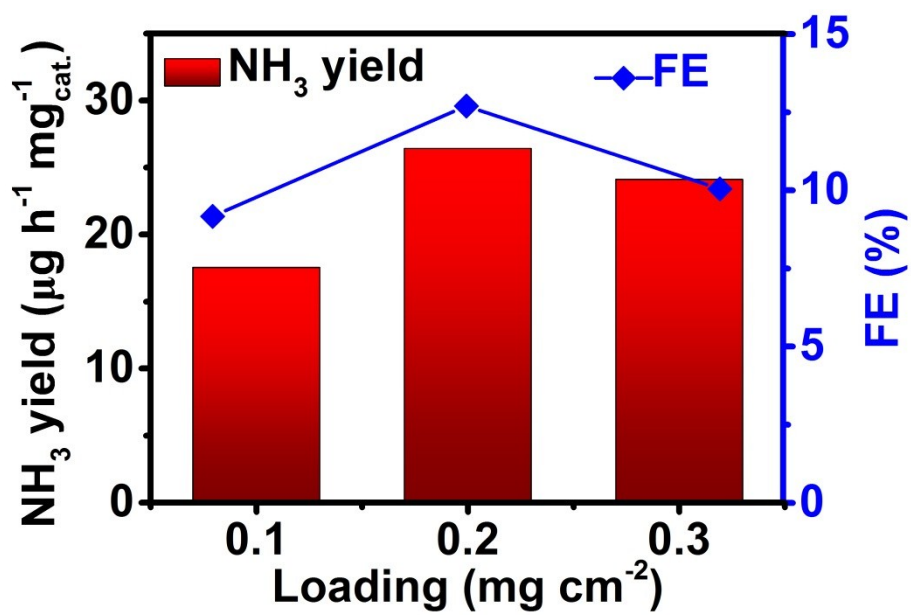


Fig. S5. NH_3 yields and FEs for BP/CP at -0.60 V with different loadings.

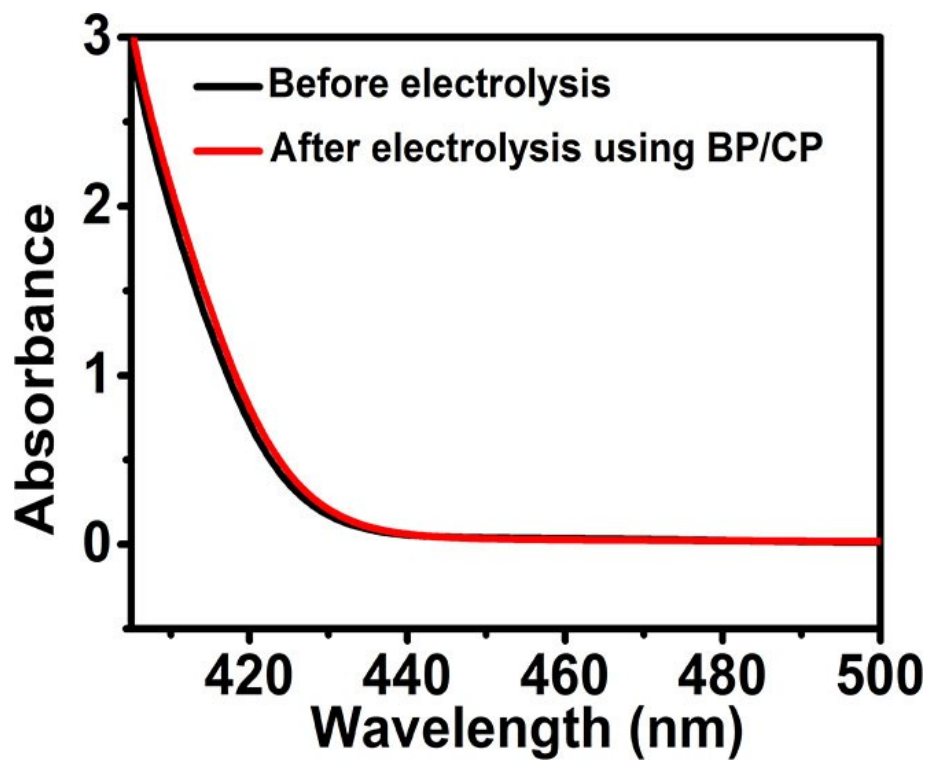


Fig. S6. UV-Vis absorption spectra of electrolytes stained with para-(dimethylamino) benzaldehyde indicator before and after 2 h electrolysis at -0.60 V.

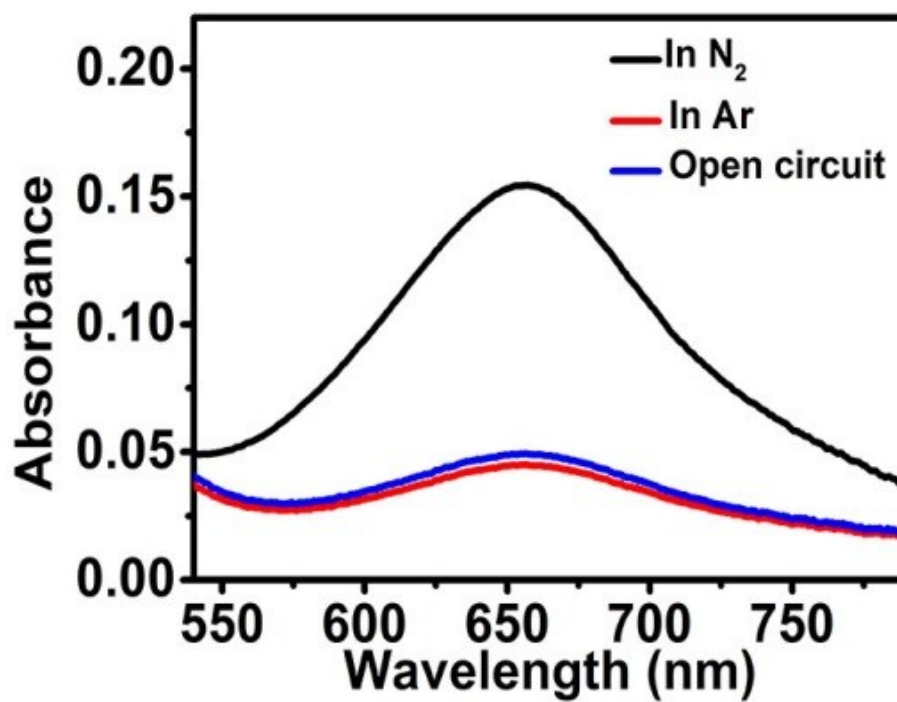


Fig. S7. UV-Vis absorption spectra of the electrolytes stained with indophenol indicator after 2 h electrolysis at -0.60 V under different electrochemical conditions.

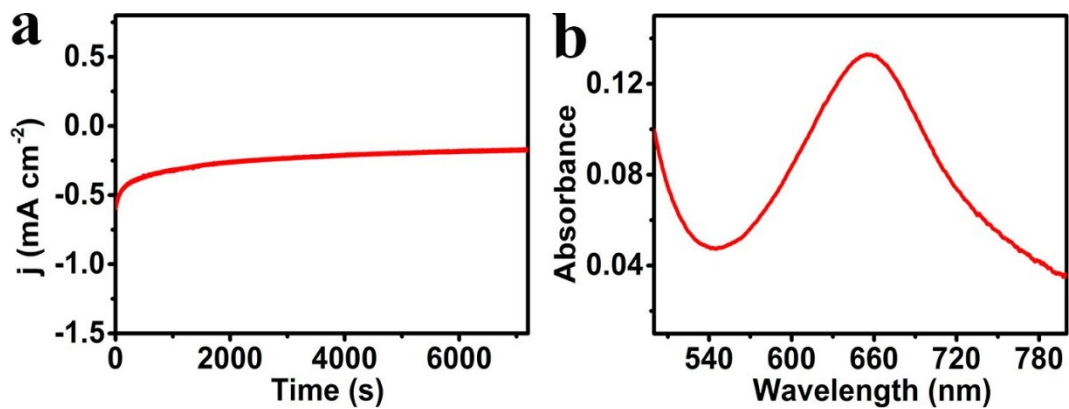


Fig. S8. (a) Time-dependent current density curves over at -0.60 V for 2 h using BP/CP after 24-h electrolysis. (b) UV-Vis absorption spectra of the electrolytes colored with indophenol indicator in no-light environment for 2 h.

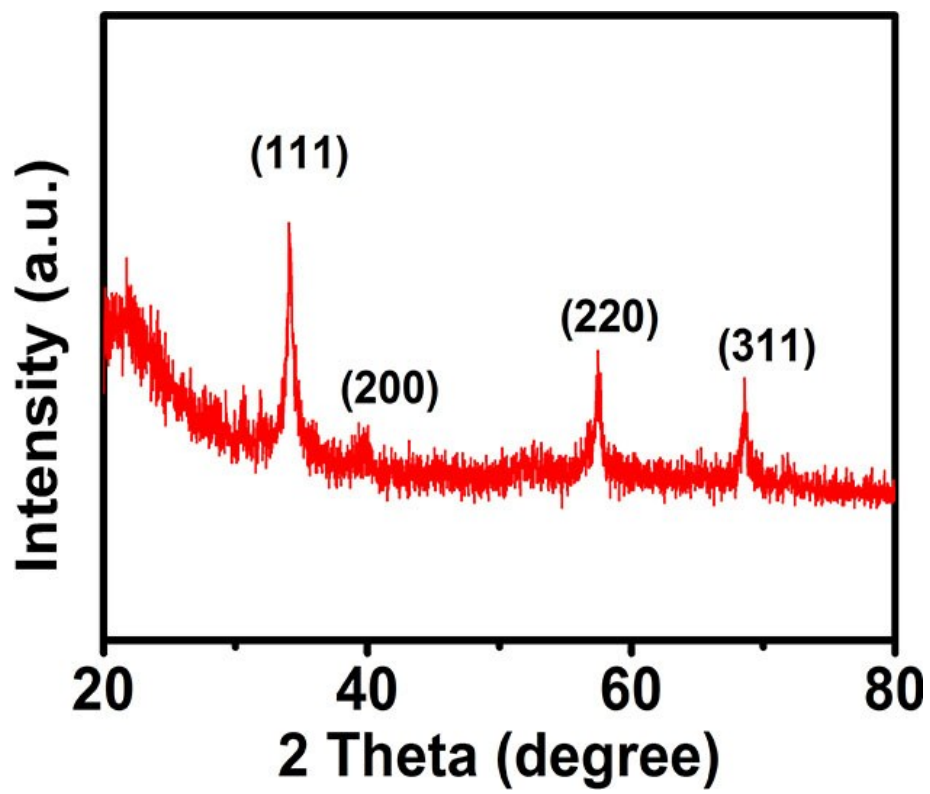


Fig. S9. XRD pattern of BP after stability test.

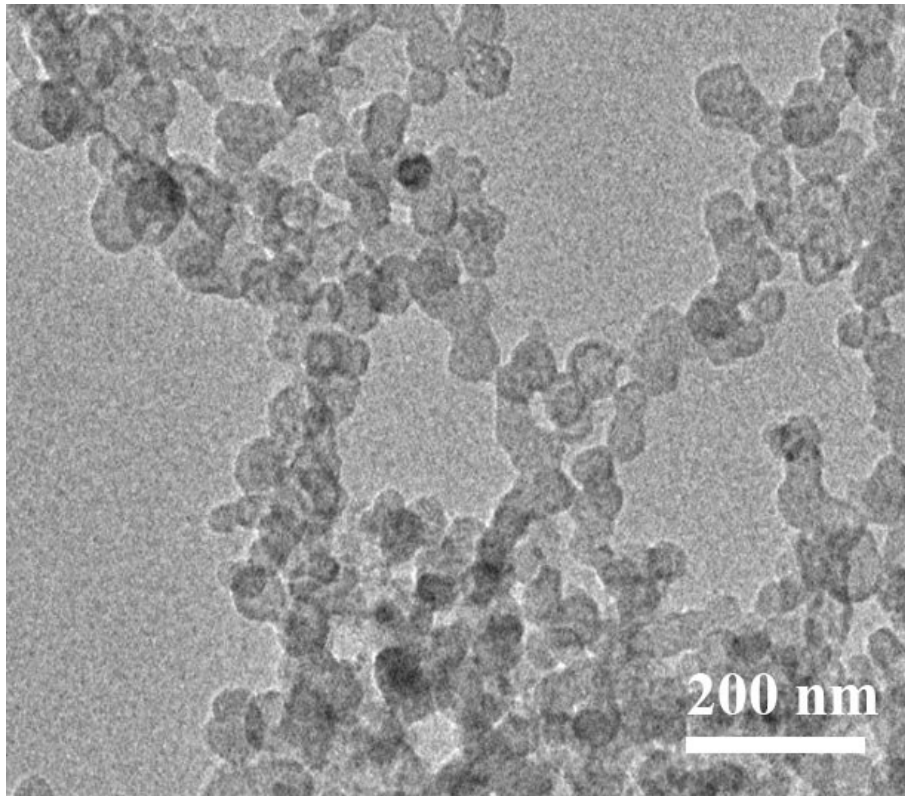


Fig.

S10.

TEM image of BP nanoparticles after stability test.

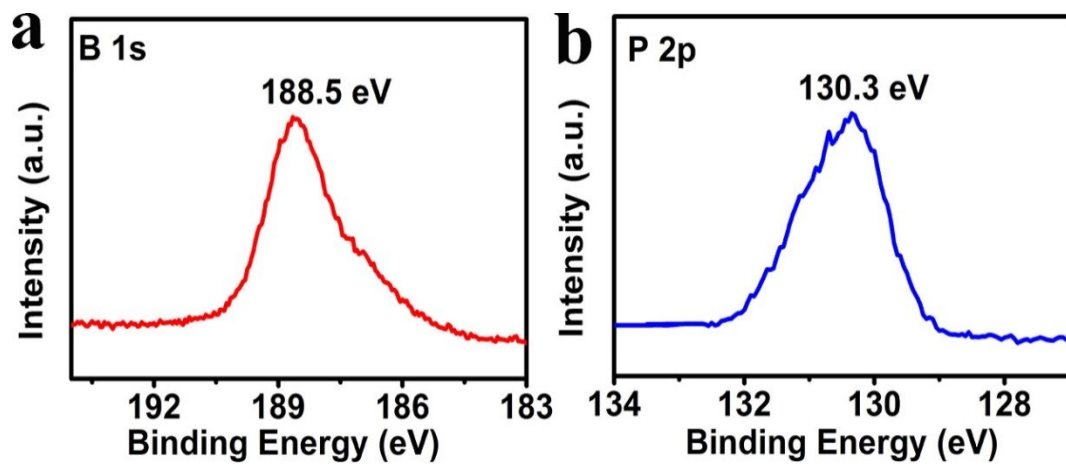


Fig. S11. XPS spectra of BP in the (a) B 1s and (b) P 2p regions after stability test.

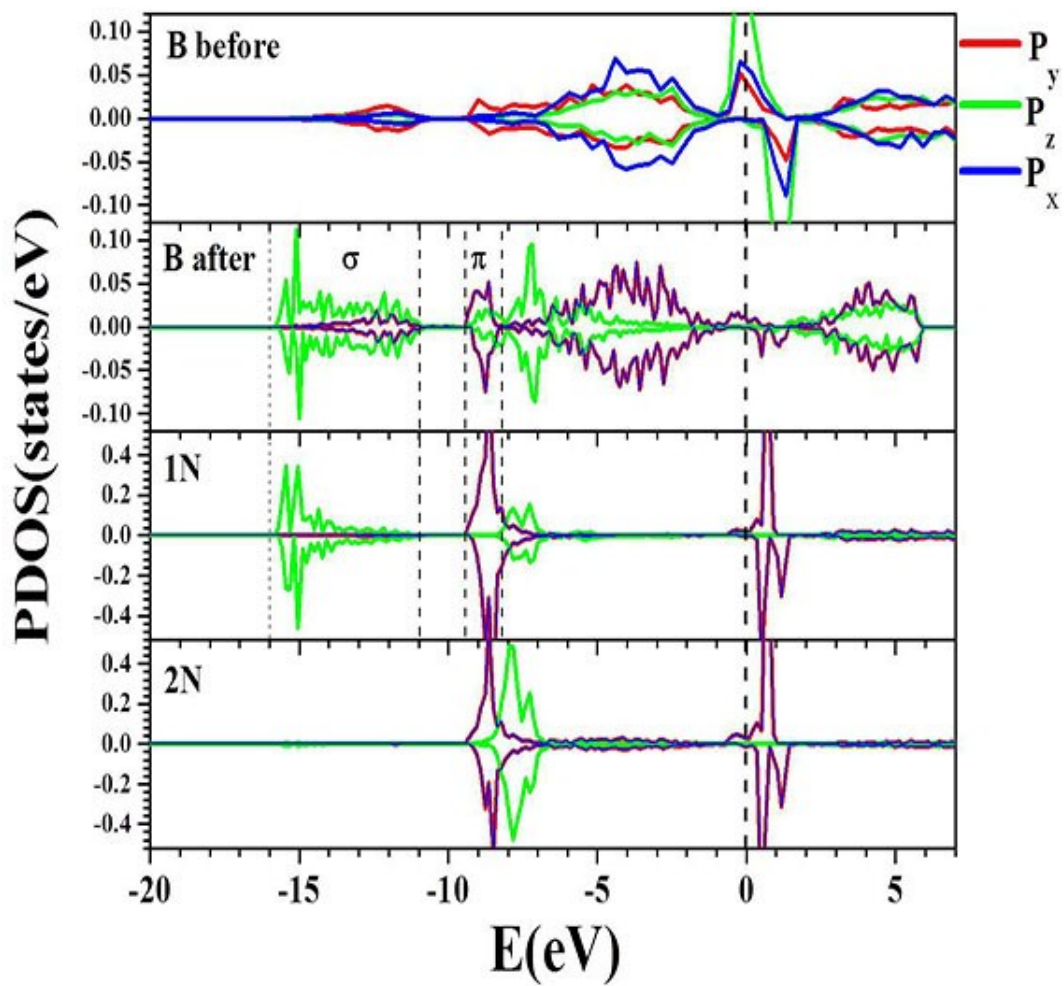


Fig. S12. DOS of B active site before and after N_2 adsorption in BP (111) surface.

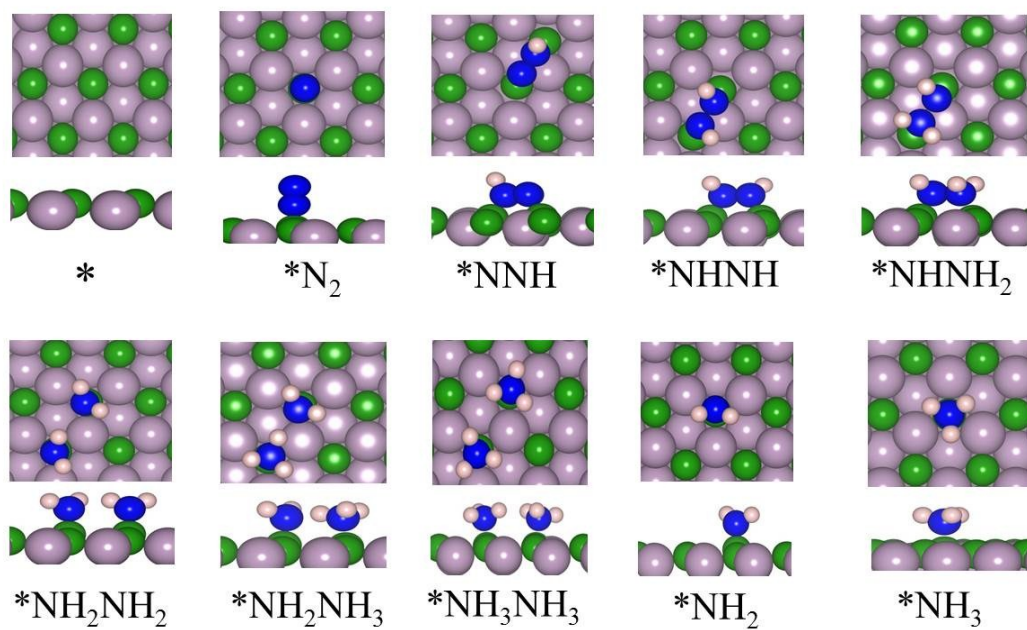
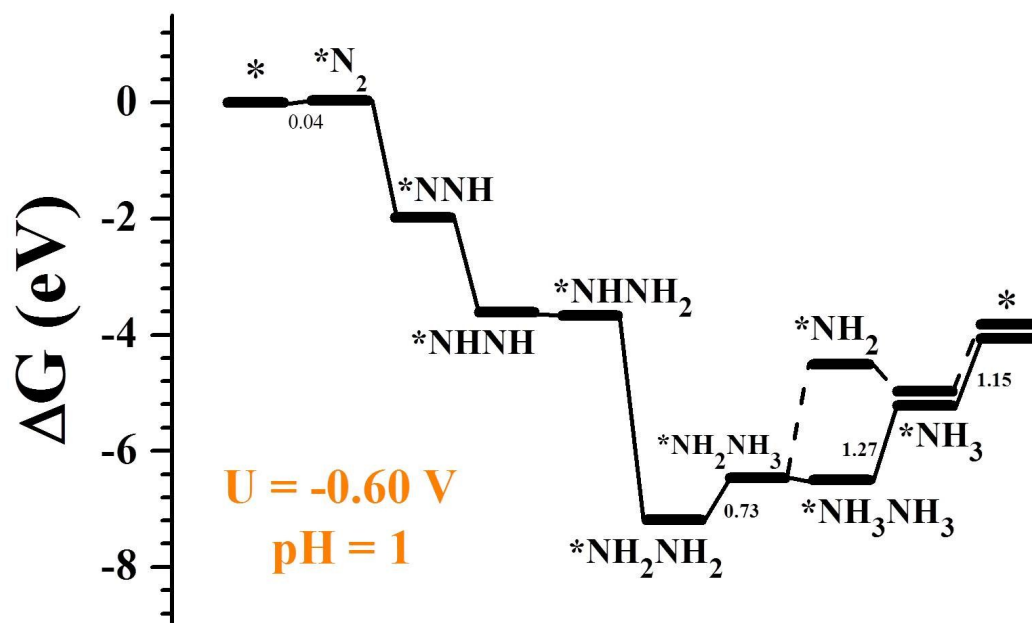


Fig. S13. Atom configurations for NRR on B (111) surface.



Reaction Pathways

Fig. S14. Free energy diagram of NRR on BP (200) surface at -0.60 V.

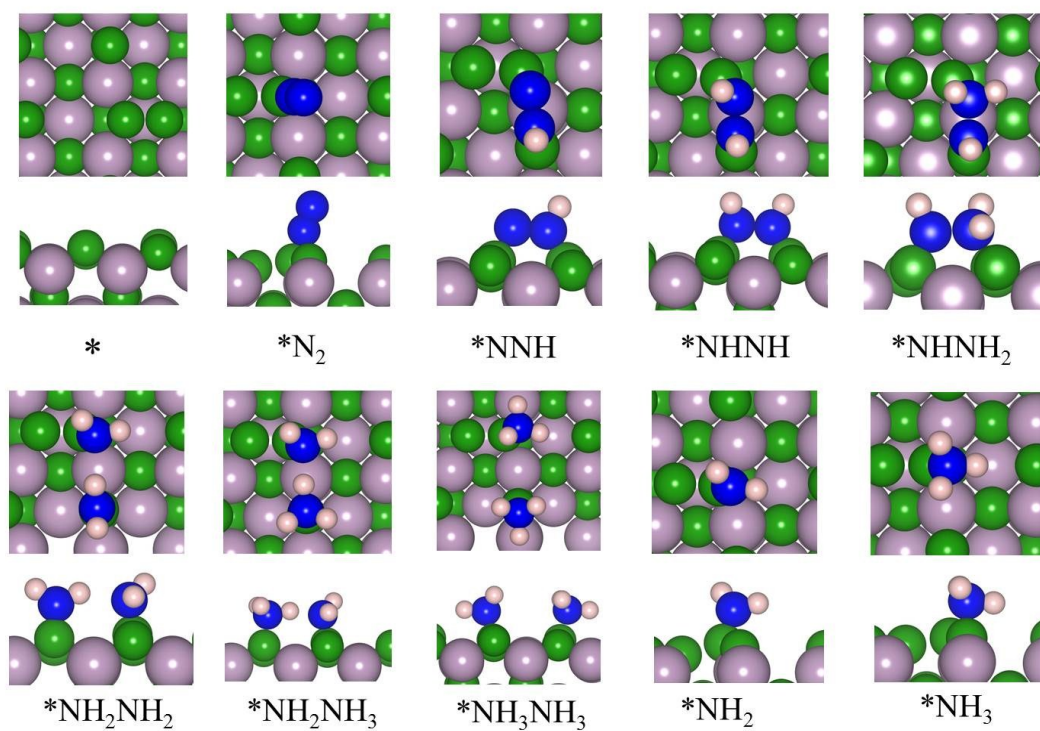
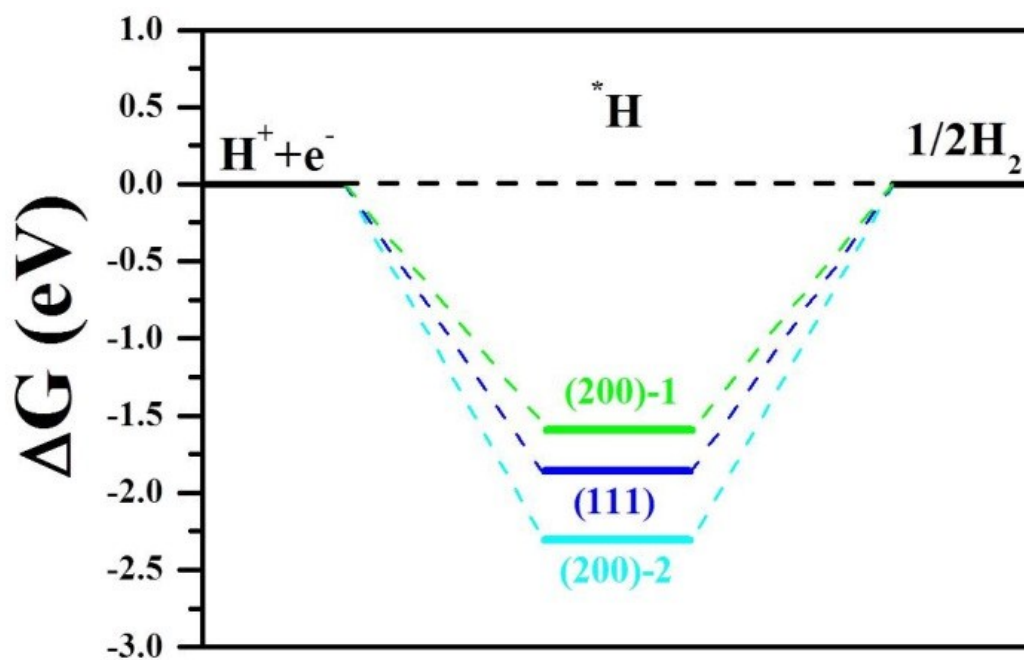


Fig. S15. Atom configurations for NRR on B (200) surface.



Reaction Pathways

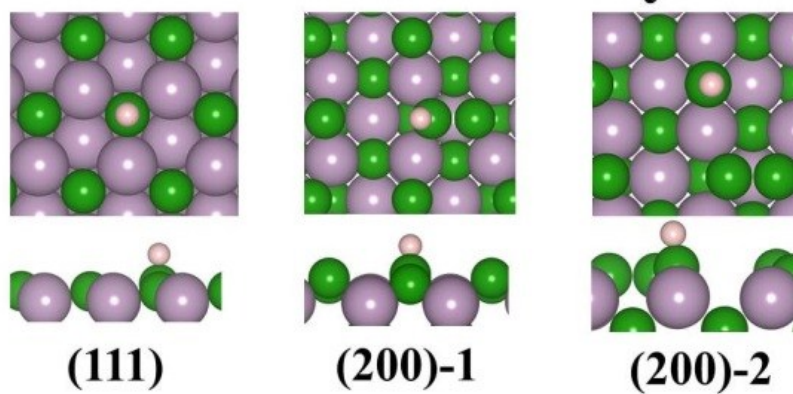


Fig. S16. HER on BP (111) and (200) surfaces.

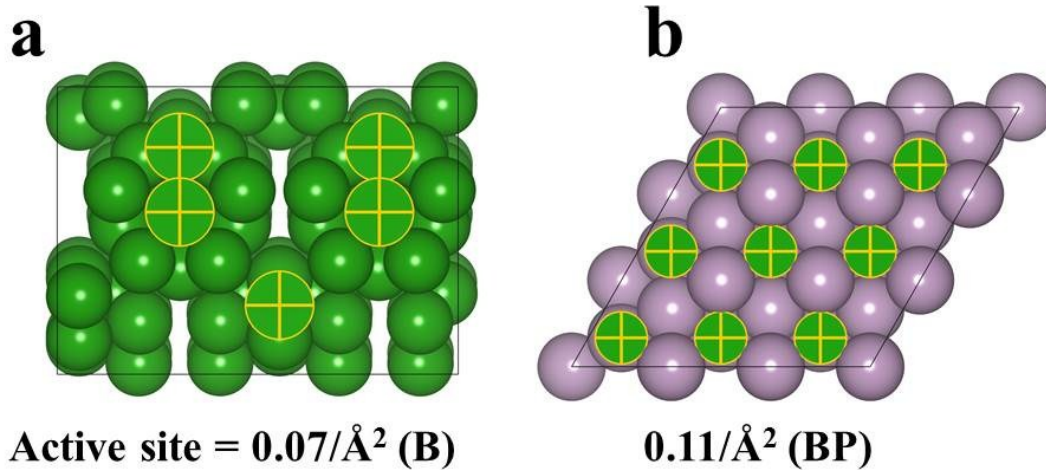


Fig. S17. Densities of active site on (a) elementary B and (b) BP. The cross represents active site.

Table S1. Comparison of the catalytic performances of non-metal NRR electrocatalysts at ambient conditions in aqueous electrolytes.

Testing method	Catalyst	Electrolyte	NH ₃ yield	FE(%)	Ref.
Indophenol blue method	BP nanoparticles	0.1 M HCl	26.42 $\mu\text{g h}^{-1} \text{mg}^{-1}_{\text{cat.}}$	12.7	This work
	boron nanosheet	0.1 M Na ₂ SO ₄	13.22 $\mu\text{g h}^{-1} \text{mg}^{-1}_{\text{cat.}}$	4.04	8
	boron nanosheet	0.1 M HCl	3.12 $\mu\text{g h}^{-1} \text{mg}^{-1}_{\text{cat.}}$	4.84	9
	defect-rich fluorographene	0.1 M Na ₂ SO ₄	9.3 $\mu\text{g h}^{-1} \text{mg}^{-1}_{\text{cat.}}$	4.2	10
	BN	0.1 M HCl	22.4 $\mu\text{g h}^{-1} \text{mg}^{-1}_{\text{cat.}}$	4.7	11
	oxygen-doped carbon nanosheet	0.1 M HCl	20.15 $\mu\text{g h}^{-1} \text{mg}^{-1}_{\text{cat.}}$	4.97	12
	black P nanosheets	0.01 M HCl	31.37 $\mu\text{g h}^{-1} \text{mg}^{-1}_{\text{cat.}}$	5.07	13
	PTCA-rGO	0.1 M HCl	24.7 $\mu\text{g h}^{-1} \text{mg}^{-1}_{\text{cat.}}$	6.9	14
	sulfur dots-graphene nanohybrid	0.5 M LiClO ₄	28.56 $\mu\text{g h}^{-1} \text{mg}^{-1}_{\text{cat.}}$	7.07	15
	S-doped carbon nanosphere	0.1 M Na ₂ SO ₄	19.07 $\mu\text{g h}^{-1} \text{mg}^{-1}_{\text{cat.}}$	7.47	16
	oxygen-doped hollow carbon microtubes	0.1 M HCl	25.12 $\mu\text{g h}^{-1} \text{mg}^{-1}_{\text{cat.}}$	9.1	17
	NPC	0.005 M H ₂ SO ₄	1.31 $\text{mmol h}^{-1} \text{g}^{-1}_{\text{cat.}}$	9.98	18
	B-doped graphene	0.05 M H ₂ SO ₄	9.8 $\mu\text{g h}^{-1} \text{cm}^{-2}$	10.8	19
	sulfur-doped graphene	0.1 M HCl	27.3 $\mu\text{g h}^{-1} \text{cm}^{-2}$	11.5	20
	PCN	0.1 M HCl	8.09 $\mu\text{g h}^{-1} \text{mg}^{-1}_{\text{cat.}}$	11.59	21
B ₄ C	0.1 M HCl	26.57 $\mu\text{g h}^{-1} \text{mg}^{-1}_{\text{cat.}}$	15.95	22	
Nessle' reagent	N-doped porous carbon	0.05 M H ₂ SO ₄	23.8 $\mu\text{g h}^{-1} \text{mg}^{-1}_{\text{cat.}}$	1.42	23
EPA Standard Method	CNS	0.25 M LiClO ₄	97.18 $\mu\text{g h}^{-1} \text{cm}^{-2}$	11.56	24

References

- 1 D. Zhu, L. Zhang, R. E. Ruther and R. J. Hamers, *Nat. Mater.*, 2013, **12**, 836–841.
- 2 G. W. Watt and J. D. Chrisp, *Anal. Chem.*, 1952, **24**, 2006–2008.
- 3 G. Kresse and J. Furthmüller, *Comp. Mater. Sci.*, 1996, **6**, 15–50.
- 4 G. Kresse and J. Furthmüller, *Phys. Rev. B*, 1996, **54**, 11169.
- 5 J. P. Perdew, K. Burke and M. Ernzerhof, *Phys. Rev. Lett.*, 1996, **77**, 3865.
- 6 S. Grimme, J. Antony, S. Ehrlich and H. Krieg, *J. Chem. Phys.*, 2010, **132**, 154104.
- 7 L. Yang, T. Wu, R. Zhang, H. Zhou, L. Xia, X. Shi and X. Sun, *Nanoscale*, 2019, **11**, 1555–1562.
- 8 X. Zhang, T. Wu, H. Wang, R. Zhao, H. Chen, T. Wang, P. Wei, Y. Luo, Y. Zhang and X. Sun, *ACS Catal.*, 2019, **9**, 4609–4615.
- 9 Q. Fan, C. Choi, C. Yan, Y. Liu, J. Qiu, S. Hong, Y. Jung and Z. Sun, *Chem. Commun.*, 2019, **55**, 4246–4249.
- 10 J. Zhao, J. Yang, L. Ji, H. Wang, H. Chen, Z. Niu, Q. Liu, T. Li, G. Cui and X. Sun, *Chem. Commun.*, 2019, **55**, 4266–4269.
- 11 Y. Zhang, H. Du, Y. Ma, L. Ji, H. Guo, Z. Tian, H. Chen, H. Huang, G. Cui, A. M. Asiri, F. Qu, L. Chen and X. Sun, *Nano Res.*, 2019, **12**, 919–924.
- 12 R. Zhang, J. Han, B. Zheng, X. Shi, A. M. Asiri and X. Sun, *Inorg. Chem. Front.*, 2019, **6**, 391–395.
- 13 L. Zhang, L. Ding, G. Chen, X. Yang and H. Wang, *Angew. Chem., Int. Ed.*, 2019, **131**, 2638–2642.
- 14 P. Li, J. Wang, H. Chen, X. Sun, J. You, S. Liu, Y. Zhang, M. Liu, X. Niu, Y. Luo, *J. Mater. Chem. A*, 2019, **7**, 12446–12450.
- 15 H. Chen, X. Zhu, H. Huang, H. Wang, T. Wang, R. Zhao, H. Zheng, A. M. Asiri, Y. Luo and X. Sun, *Chem. Commun.*, 2019, **55**, 3152–3155.
- 16 L. Xia, X. Wu, Y. Wang, Z. Niu, Q. Liu, T. Li, X. Shi, A. M. Asiri and X. Sun, *Small Methods*, 2018, **14**, 1800251.
- 17 T. Wu, P. Li, H. Wang, R. Zhao, Q. Zhou, W. Kong, M. Liu, Y. Zhang, X. Sun and Feng Gong, *Chem. Commun.*, 2019, **55**, 2684–2687.
- 18 C. Zhao, S. Zhang, M. Han, X. Zhang, Y. Liu, W. Li, C. Chen, G. Wang, H. Zhang and H. Zhao, *ACS Energy Lett.*, 2019, **4**, 377–383.

- 19 X. Yu, P. Han, Z. Wei, L. Huang, Z. Gu, S. Peng, J. Ma and G. Zheng, *Joule*, 2018, **2**, 1610–1622.
- 20 L. Xia, J. Yang, H. Wang, R. Zhao, H. Chen, W. Fang, A. M. Asiri, F. Xie, G. Cui and X. Sun, *Chem. Commun.*, 2019, **55**, 3371–3374.
- 21 C. Lv, Y. Qian, C. Yan, Y. Ding, Y. Liu, G. Chen and G. Yu, *Angew. Chem., Int. Ed.*, 2018, **57**, 10246–10250.
- 22 W. Qiu, X. Xie, J. Qiu, W. Fang, R. Liang, X. Ren, X. Ji, G. Cui, A. M. Asiri, G. Cui, B. Tang and X. Sun, *Nat. Commun.*, 2018, **9**, 3485.
- 23 Y. Liu, Y. Su, X. Quan, X. Fan, S. Chen, H. Yu, H. Zhao, Y. Zhang and J. Zhao, *ACS Catal.*, 2018, **8**, 1186–1191.
- 24 Y. Song, D. Johnson, R. Peng, D. K. Hensley, P. V. Bonnesen, L. Liang, J. Huang, F. Yang, F. Zhang, R. Qiao, A. P. Baddorf, T. J. Tschaplinski, N. L. Engle, M. C. Hatzell, Z. Wu, D. A. Cullen, H. M. Meyer III, B. G. Sumpter and A. J. Rondinone, *Sci. Adv.*, 2018, **4**, e1700336.